Combined use of rheology and portable low-field NMR in cystic fibrosis patients

Michela Abrami [a], Massimo Maschio [b], Massimo Conese [c], Marco Confalonieri [d], Fabio Gerin [a], Barbara Dapas [e], Rossella Farra [f], Alessandra Adrover [g], Lucio Torelli [f], Barbara Ruaro [d], Gabriele Grassi [e,*], Mario Grassi [a]

[a] Department of Engineering and Architecture, University of Trieste, Via Valerio 6/A, I-34127, Trieste, Italy
[b] Institute for Maternal and Child Health, IRCCS Burlo Garofolo, Via Dell'Istria, 65, I-34137, Trieste, Italy
[c] Department of Medical and Surgical Sciences, Foggia University, Ospedali Riuniti, Via L. Pinto, 1, I-71122, Foggia, Italy
[d] Cattinara University Hospital, Pulmonology Department, Strada di Fiume 447, I-34149, Trieste, Italy
[e] Department of Life Sciences, Cattinara University Hospital, Trieste University, Strada di Fiume 447, I-34149, Trieste, Italy
[f] Clinical Department of Medical, Surgical and Health Sciences, Cattinara University Hospital, Trieste University, Strada di Fiume 447, I-34149, Trieste, Italy
[g] Department of Chemical Engineering, Materials and Environment, Sapienza University of Roma, Via Eudossiana 18, I-00184, Rome, Italy

ARTICLE INFO

Keywords:
Cystic fibrosis
Rheology
Low field NMR
Sputum

ABSTRACT

Background: As most cystic fibrosis (*CF*) patients progress to respiratory failure, lung functionality assessment is pivotal. We previously developed a test that indirectly monitors airways (inflammation/functional test) by measuring the spin-spin relaxation time (T_{2m}) of the water hydrogens present in *CF* sputum. Here the T_{2m} significance in the monitoring of *CF* lung disease was further investigated by studying the correlation of T_{2m} with: 1) sputum viscoelasticity, 2) mucociliary clearability index (*MCI*)/cough clearability index (*CCI*) and 3) sputum average mesh-size.

Methods: Sputum samples from 25 consenting *CF* subjects were analyzed by rheology tests (elastic modulus *G* and zero shear viscosity η_0) and Low Field Nuclear Magnetic (*LF-NMR*) resonance (T_{2m}). *MCI/CCI* were calculated from the rheological parameters. The average mesh-size (ξ) of the sputum structure was then evaluated by rheology/*LF-NMR*, together with FEV_1 for each patient.

Results: There was an inverse correlation between *G* and η_0 versus T_{2m}, indicating that a worsening of the lung condition (T_{2m}-FEV_1 drop) is paralleled by an increase in sputum viscoelasticity (*G* and η_0) favoring mucus stasis/inflammation. A direct correlation was also observed between T_{2m} and *MCI/CCI*, showing that T_{2m} provides information as to airway mucus clearing. Moreover, there was a direct correlation between T_{2m} and the average sputum mesh size (ξ).

Conclusions: We demonstrated a correlation between T_{2m} (measured in *CF* patient's sputum) and the sputum viscoelasticity/average mesh-size and with *MCI/CCI*, parameters related to airway mucus clearing. Thus, the present data strengthen the potential of our test to provide indirect monitoring of airway disease course in *CF* patients as T_{2m} depends on mucus solid concentration and nanostructure.

1. Introduction

Cystic fibrosis (*CF*) is an autosomal recessive disease caused by mutations in the gene encoding of the cystic fibrosis transmembrane conductance regulator (*CFTR*) [1,2] responsible for chloride and sodium ion exchange across epithelial membranes. Dysfunctional *CFTR* induces the production of thick/viscous mucoid secretions in multiple organs, in particular the airways, where an augmented mucus viscosity [3,4] is determined by the pathological increase in proteins, mucin and biological polymers [5]. This process impairs mucociliary clearance, promoting inflammation and bacterial infection [6]. Chronic inflammation can lead to airway remodeling, which, in turn, may progress to respiratory failure, the most common cause of death for *CF* patients [7]. Therefore, as sputum is a rich and noninvasive source of biomarkers of inflammation/infection, the determination of sputum properties is a relevant parameter able to indirectly monitor lung disease.

* Corresponding author.
E-mail address: ggrassi@units.it (G. Grassi).

Accepted 20 September 2021

Recently [8,9], we studied the characteristics of *CF* sputum using low field nuclear magnetic resonance (*LF-NMR*). Expectorated sputum is easily obtained from patients and its properties mirror those of mucus [5,10]. The *LF-NMR* technique we used allows for the measurement of the spin-spin relaxation time (T_{2m}) of the water hydrogens present in the *CF* sputum. Our previous data showed [8,9] that the T_{2m} measured in *CF* sputum has an indirect correlation with circulating/local inflammation markers and a direct correlation with FEV_1 (forced expiratory volume in the first second, i.e. the amount that is exhaled in the first second purposefully trying to breath out as much air as possible), the most commonly used test in clinical practice for the evaluation of lung function [11]. Together, our previous findings, suggest that the assessment of physical properties of sputum by T_{2m}, may well provide a useful tool for the indirect monitoring of lung disease in *CF* patients. Indeed, as it will be discussed in this paper, T_{2m} can provide information about sputum nano-structure that the determination of solid concentration cannot.

The main objective of this study was to further investigate the role T_{2m} plays in the monitoring of lung disease in *CF* patients. To this aim investigations were carried out to determine as to any possible correlation between T_{2m} and sputum viscoelasticity as several authors have reported a relationship between sputum viscoelasticity and the severity of lung pathology [12–17]. Moreover, Odeblad et al. used *LF-NMR* and rheology to study the properties of lung mucus [18,19].

A secondary objective was that of investigating whether there was any correlation between T_{2m} and both the mucociliary clearability index (*MCI*) and the cough clearability index (*CCI*). *MCI* and *CCI,* which can be calculated from the rheological properties in sputum, as reported by King et al. [20,21], represent the two main mucus clearance mechanisms. In healthy subjects, proper *MCI/CCI* allows for mucus clearance from the airways, preventing mucus stasis and, consequently, bacterial infection/inflammation. In *CF* subjects, the reduction in *MCI/CCI* is a relevant finding as it reflects the severity of lung pathology. In this regard, Ma et al. [13], studied the rheology of *CF* sputum and measured mucociliary clearability and cough clearability showing that sputum viscoelastic properties are tightly associated with lung function and disease status. The study of Ma et al. was lead on a per patient basis and a trend in a cross-population analysis was not found.

As last objective of this work, relying on the Flory theory [22] and on the rheological data, we estimate the sputum average mesh size ξ, a parameter useful to predict drug diffusion (and thus effectiveness) through mucus whose permeability to drugs is known to decrease with its viscoelastic properties [23].

Therefore, in this work, the possible correlation between T_{2m} and sputum viscoelasticity/*MCI/CCI*/sputum-average mesh size was assessed, for the first time, by a combined analysis based on rheology and *LF-NMR*. This novel approach provided information as to the macro- (viscosity, elasticity, average magnetic relaxation time) and micro-scale (mesh size distribution) characteristics of *CF* sputum.

2. Materials and methods

2.1. Sample collection

Sputum samples from 25 CF patients (a mix of clinical status) were provided by the Burlo Garofolo Hospital, following a procedure approved by the Ethics Committee (prot n. 496/2916, CI M − 11, 22-3-2016). Written informed consent was obtained from each patient. One sputum specimen was collected before a chest physiotherapy session in randomly selected adult and young patients (see Table 1) able to expectorate. Non-expectorant patients were excluded, as were subjects ≤7 years of age. The only exception was patient n.10 (Table 1) where three samples were taken into consideration so as to study the time evolution over a 3 months period. However, only the first sample was considered in the statistical analyses. The samples of healthy subjects reported in Fig. 1 were obtained from published papers [24].

So as to evaluate any correlation among the sputum shear modulus *G*, zero-shear viscosity η_0, average magnetic relaxation time T_{2m} and FEV_1 in a broad range of FEV_1 values, patients with a large uniform FEV_1 distribution (from ≈31% to 85%, see also Table 1) were selected. The aforementioned criteria allowed for the recruitment of most patients who attended Burlo Garofolo Hospital for a clinical visit during our study period (from May 2019 to June 2020). Spontaneously expectorated (1–2 ml) sputum was collected from *CF* patients in sterile cups and immediately used for T_{2m} determination. The samples were then transferred from the *LF-NMR* glass tube to a rheometer device for analysis.

Table 1
Patient characteristics and therapies.

n°	I mut	II mut	sex	age	FEV_1	Therapies
1	F508del	N1303K	M	42	80	minocycline + levofloxacin
2	F508del	I507del	M	36	64	colistimethate
3	F508del	711+5G- > A	M	44	61	ciproxin + prednisone
4	F508del	F508del	F	15	82	azithromycin + prednisone + minocycline
5	G542X	deltaI507	F	18	85	colistin + azithromycin
6	F508del	2,3del(21 kb)	M	37	79	prednisone
7	F508del	1677delTA	M	34	62	Minocin + cysteamine
8	621+1G- > T	2347delG	M	36	79	levofloxacin
9	F508del	3659delC	F	49	47	No antibiotic therapy
10	F508del	F508del	F	23	34	levofloxacin
11	1717-1G > A	1717-1G > A	M	27	71	prednisone + azithromycin + ceftazidime
12					67	amikacin + imipenem + cefoxitin
13	F508del	3120+1kbdel8,6k	M	35	59	levofloxacin
14	F508del	F508del	F	33	31	prednisone + ciprofloxacin + minocycline + itraconazole + aerosol amikacin
15	G542X	G542X	F	31	65	prednisone + levofloxacin
16	F508del	F508del	M	21	38	prednisone + ciprofloxacin + minocycline + itraconazole + aerosol amikacin
17	F508del	F508del	F	37	67	levofloxacin
18	N1303K	G542X	M	27	37	levofloxacin + prednisone + colistimethate
19	F508del	N1303K	F	34	43	prednisone + ciprofloxacin + minocycline + itraconazole + tobramycin
20	F508del	F508del	F	25	46	temocillin + amikacin + prednisone + sodium colistimethate
21	F508del	4382delA	F	56	57	Bactrim (sulfamethoxazole + trimethoprim ratio 5:1)
22	F508del	F508del	F	26	66	levofloxacin
23	R1162X	1717-1G- > A	M	43	40	prednisone + bactrim + levofloxacin
24	F508del	F508del	M	43	41	prednisone + + ciprofloxacin + sodium colistimethate
25	F508del	2368-69del11	F	20	49	+ ciprofloxacin + prednisone

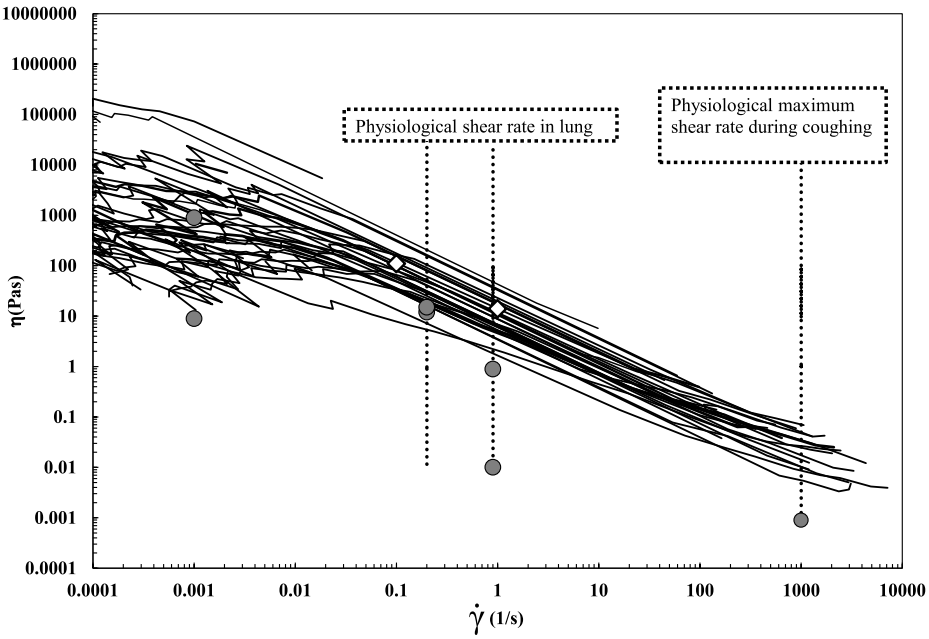

Fig. 1. Viscosity (η) dependence on shear rate ($\dot{\gamma}$) referring to our CF sputum samples (black lines) and literature data referring to healthy human mucus (grey circles) [40] and *CF* sputum (white diamonds) [24] evaluated at physiological shear rates (healthy lung [24] and the maximum shear rate reached during coughing [40]).

2.2. Rheology

Rheology is used to describe and assess the flow behavior of materials. Fluids flow at different speeds and solids can be deformed to a certain extent. Depending on their physical behavior, materials can be put into liquids on one side and solids on the other. Rheological measurements, including viscosity (resistance to flow) and elasticity (stiffness), are often used together to describe the consistency of mucus. The rheological properties of mucus vary as a function of shear stress, time scale (rate) of shearing, and length scale. Changes in the rheological properties of mucus may greatly affect its ability to function as a lubricant, selective barrier, and the body's first line of defense against infection. In addition, the rheological characterization can provide insight into the nanostructure of a gel-like material such as mucus/sputum.

The viscoelastic properties of the analyzed samples were determined by three typical rheological tests, i.e. the stress sweep, frequency sweep and steady value test. While stress sweep tests serve to detect the maximum deformation the sample can undergo without altering its internal micro-nano-structure, frequency sweep tests determine how much the elastic (G') and viscous (G'') properties (moduli) of the sample depend on solicitation pulsation ω. Relying on G' and G'' knowledge, the shear modulus G of the sample was determined as previously described [25,26] and as detailed in supporting information S1. Then, knowing G, Flory theory [22] and the equivalent network theory [27] allow to evaluate the average mesh size ξ of the polymeric network pervading *CF* sputum as explained in supporting information S1.

Interestingly, some insights as to lung functionality/inflammation can be deduced by the evaluation of the mucociliary clearability index (*MCI*) and the cough clearability index (*CCI*) [28–30] (see also supporting information S1 for further details on the determination of *MCI* and *CCI* by rheological characterization). Indeed, as many of the particles that settle on airway surfaces are infectious, airways have evolved innate defense mechanisms that constantly protect them against bacterial and other types of infection. The two major mucus clearance mechanisms from the airways are mucociliary clearance and, when it fails or is overloaded, coughing [31]. As the cilia beat at about 10–20 Hz, with an amplitude of 5 μm, mucus transport velocity (frequency * amplitude) is in the order of 1 cm/min, whilst the velocity during a cough maneuver is about 100 times greater. Therefore, low-frequency (1 rad/s) viscoelasticity measurements are appropriate for observations of mucociliary clearance, whereas high-frequency measurements (100 rad/s) are more predictive for cough clearance [32–34].

Other important information can be obtained from the steady value test (SV) that assesses the dependence of the sample shear viscosity (η) on the shear rate ($\dot{\gamma}$). The sample viscosity, evaluated in correspondence to a vanishing shear rate (zero shear viscosity η_0), is a particularly important parameter. η_0 was determined by fitting the Cross model [35] onto the *SV* data (see also supporting information S1). All rheological measurements were performed in triplicate by a stress controlled rotational rheometer (Haake Mars Rheometer, 379-0200 Thermo Electron GmbH, Karlsruhe, Germany) equipped with cone-plate geometry (C35, diameter = 35 mm). So as to avoid problems of evaporation, sputum characterization was done at +20 °C, using a glass solvent trap.

2.3. Portable low field NMR

NMR relies on the ability of hydrogen atoms dipole to react to the perturbation of an external constant magnetic field B_0, where they are embedded. Basically, after a temporary B_0 perturbation obtained by the application of a radio frequency pulse B_1, perpendicular to B_0, the dipoles tend to return to their initial alignment with B_0 (relaxation). Relaxation rate is expressed by the inverse of a characteristic time constant T_2 called spin-spin or transverse relaxation time [36]. The relaxation process (signal amplitude decay $I(t)$, t = time) can be described by the sum of m exponential terms, each one characterized by a different time decay constant (T_{2i}) and weight ($A_{i\%}$; $[A_{1\%} + A_{2\%} + \ldots A_{m\%} = 100]$) [37]. This allows for the evaluation of the average relaxation time (T_{2m}) and the inverse relaxation time ($(1/T_2)_m$, as detailed in supporting information S2. Interestingly, at each relaxation time T_{2i} corresponds a mesh of size ξ_i, as reported in supporting information S2 and in Refs. [36–38].

LF-NMR measurements were taken at +37 °C, by a Bruker Minispec mq20 (0.47 T, Germany, Figure S1). The T_{2m} determination was performed according to the CPMG sequence (Carr–Purcell–Meiboom–Gill) [39] {90°[-τ-180°-τ(echo)]n-T_R} with a 8.36 μs wide 90°pulse, τ = 250 μs and a T_R (sequence repetition rate) equal to 5 s. Each spin-echo decay had n points and was repeated 36 times (number of scans).

2.4. Statistical analysis

The nature of the experimental data distribution (normal or not) was assessed by the Kolmogorov-Smirnov test (KS-test). Based on the KS-test results, the Spearman's correlation coefficient (r_{sp}) verified direct or inverse correlations amongst *G*, η_0, T_{2m}, FEV_1, *MCI* and *CCI*. Any *p*-values below 0.05 were considered statistically significant.

Principal component analysis (PCA) on the variance/covariance matrix as well as on the correlation matrix was performed to assess the strength of the correlation among the different variables. 95% confidence ellipse from the covariance matrix of bivariate data was evaluated to better visualize direct or inverse correlations and to identify bivariate outliers. The axes of the ellipse are oriented along the eigenvectors of the covariance matrix and their lengths are proportional to the square root of the corresponding eigenvalues times a factor 1.96, corresponding to a 95% confidence interval for a normal distribution.

3. Results

3.1. Rheological and LF-NMR characterization of sputum

The flow properties of the *CF* sputum collected in this study were compared to those of healthy subjects' sputum and patients obtained from published papers. Fig. 1 shows the comparison among the viscosity (flow curves, black lines) of our *CF* sputum samples with the viscosity of healthy mucus (grey circles) [40] and *CF* sputa (white diamonds) obtained from previously published data [24] and evaluated in correspondence to typical shear rates ($\dot{\gamma}$) in healthy lungs ($\dot{\gamma} = 10^{-1}$-10^{0} 1/s) [24] and during coughing ($\dot{\gamma}_{max} = 10^{3}$-$10^{4}$ 1/s) [40].

The viscosity of the *CF* sputa was considerably higher than that of healthy mucus along all the shear rate range, in agreement with literature data (white diamonds) [24].

The frequency sweep tests, shown in Fig. 2, relate to three representative samples and show the gel-like nature (or incipient gel nature) of our samples. Indeed, the data show that the elastic component (G') prevailed over the viscous one (G'') and both $G' - G''$ were almost independent of pulsation ω [25,26].

Healthy subjects' sputa essentially coincides with saliva, characterized by $G' \approx 0$. Sputum characterization was completed by *LF-NMR* analysis (Fig. 3). The data showed a signal amplitude decay ($I(t)$) for five representative samples and one healthy subject. There are evident differences in the decay curves, which depend on the increased concentration and spatial organization of the solids within the sputum. This, in turn, determines a higher sputum dehydration [8,9] and viscosity.

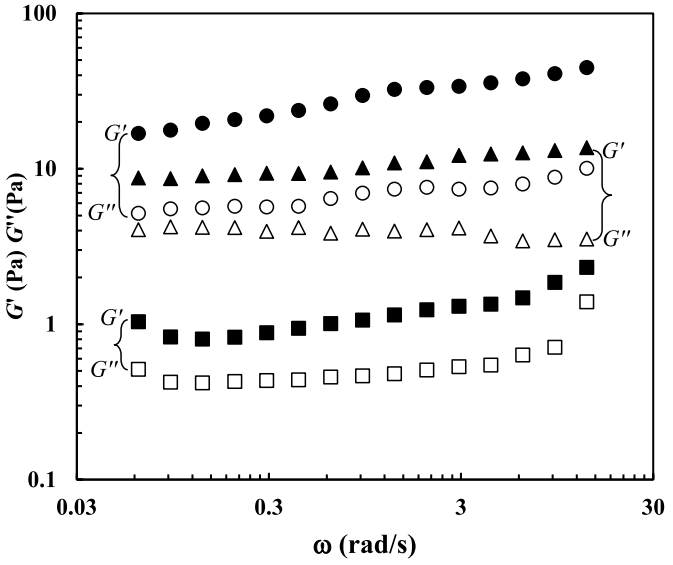

Fig. 2. Frequency sweep test. Elastic (G' - full symbols) and viscous (G'' - empty symbols) moduli dependence on pulsation ($\omega = 2\pi f$) at $\tau = 0.05$ Pa ($T = 20$ °C) referring to three representative samples. Braces help in enucleating each mechanical spectrum, i.e. the G' and G'' trends corresponding to a single patient. All the other samples fall within the values shown in the picture and are not reported to keep a good image clarity.

3.2. The relationship of the sputum rheological features with T_{2m} and FEV_1

Fig. 4A shows the inverse correlation between both the shear modulus *G* (elastic properties) and the zero shear viscosity η_0 (viscous properties) compared to T_{2m}. There is an evident link between disease worsening (a drop in T_{2m}) and the increased elastic and viscous properties of the sputum. Also FEV_1 had an inverse correlation with η_0 and *G* (Fig. 4B). Notably, the η_0 correlation with T_{2m} and FEV_1 (Fig. 4A and B) is less pronounced than that observed with *G*; this can be appreciated by the direct comparison between the 95% confidence ellipses. Moreover, the data extrapolated from Fig. 4A and B confirm our previous findings [8,9], i.e. there is a significant correlation ($r_{sp} = 0.55$, $p = 4{*}10^{-3}$) between T_{2m} and FEV_1 (correlation line: $FEV_1 = (1.7 \pm 0.5){*}10^{-2}{*}T_{2m} + (40 \pm 6)$).

3.3. The relationship between MCI and CCI with T_{2m} and FEV_1

MCI and *CCI,* which can be calculated from the rheological properties of the sputum [28–30], reassume the sputum viscoelastic features. Fig. 5A shows a direct correlation between T_{2m} and *CCI/MCI*. Our data also showed a direct correlation between *CCI/MCI* and FEV_1 (Fig. 5B), suggesting that the progressive deterioration of lung function (decline in FEV_1) occurred in parallel with a reduced mucus clearance (*CCI/MCI*) ability.

3.4. The determination of the average mesh size of sputum

The synergic combination of rheology and *LF-NMR* allows for an estimation of a very important parameter, i.e., the average mesh size (ξ) of the polymeric structure pervading the sputum of *CF* patients. It is well known that drug diffusivity inside a gel-like system depends on the ratio between the diffusing drug molecule radius and ξ [41]. The smaller this ratio, the higher the drug accessibility into mucus, enhancing its efficacy. Relying on what is presented in sections 2.2-2.3 and in supporting information S2, Fig. 6 shows the direct correlation between ξ and T_{2m}.

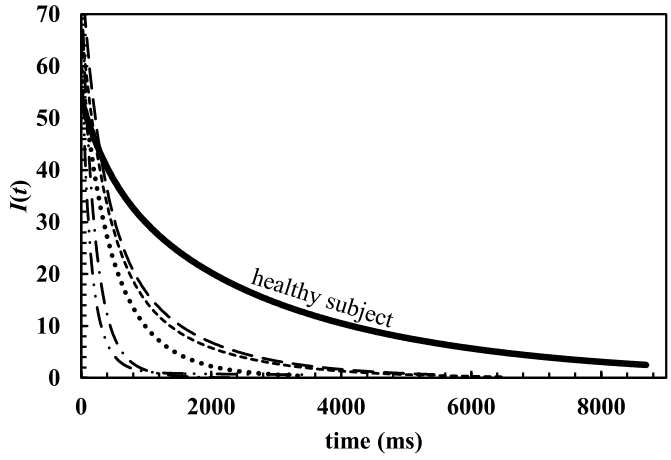

Fig. 3. Transverse magnetization reduction (I(t)) referring to five representative sputum samples from five CF patients (dashed/dotted lines), plus one referring to a healthy subject (solid line). All the other samples fall within the values shown in the picture and are not reported to keep a good image clarity.

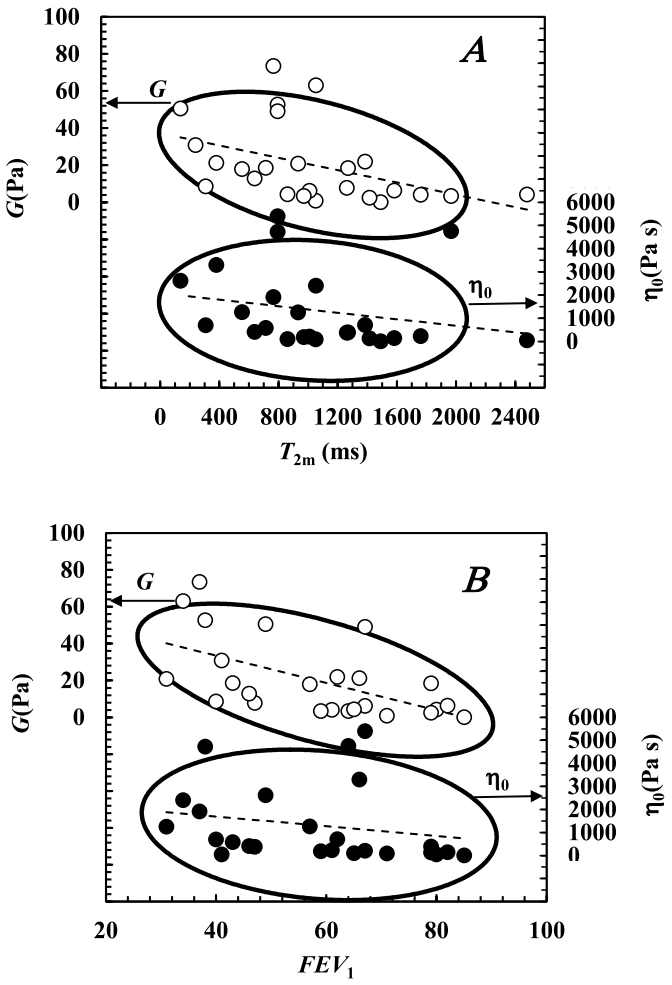

Fig. 4. A) There is a significant inverse correlation between the shear modulus G (white circles; left vertical axis, see the left oriented arrow) and the average relaxation time T_{2m} ($r_{sp} = -0.57$, $p = 3*10^{-3}$). The dashed line indicates the linear interpolant $G = -(1.6 \pm 0.7)*10^{-2}*T_{2m} + (37 \pm 8)$. There is a significant inverse correlation between the zero shear viscosity η_0 (black circles; right vertical axis, see the right oriented arrow) and the average relaxation time T_{2m} ($r_{sp} = -0.48$, $p = 1.7*10^{-2}$). The dashed line indicates the linear interpolant $\eta_0 = -(0.7 \pm 0.6)*T_{2m} + (2080 \pm 756)$ while solid lines indicate the 95% confidence ellipses. *B*) There is a significant inverse correlation between the shear modulus *G* (white circles; left vertical axis, see the left oriented arrow) and FEV_1 ($r_{sp} = -0.63$, $p = 0.8*10^{-3}$). The dashed line indicates the linear interpolant $G = -(0.74 \pm 0.2)*FEV_1 + (63 \pm 13)$. There is a significant inverse correlation between the zero shear viscosity η_0 (black circles; right vertical axis, see the right oriented arrow) and FEV_1 ($r_{sp} = -0.41$, $p = 4.6*10^{-2}$). The dashed line indicates the linear interpolant $\eta_0 = -(21 \pm 20)*FEV_1 + (2543 \pm 1275)$ while solid lines indicate the 95% confidence ellipses.

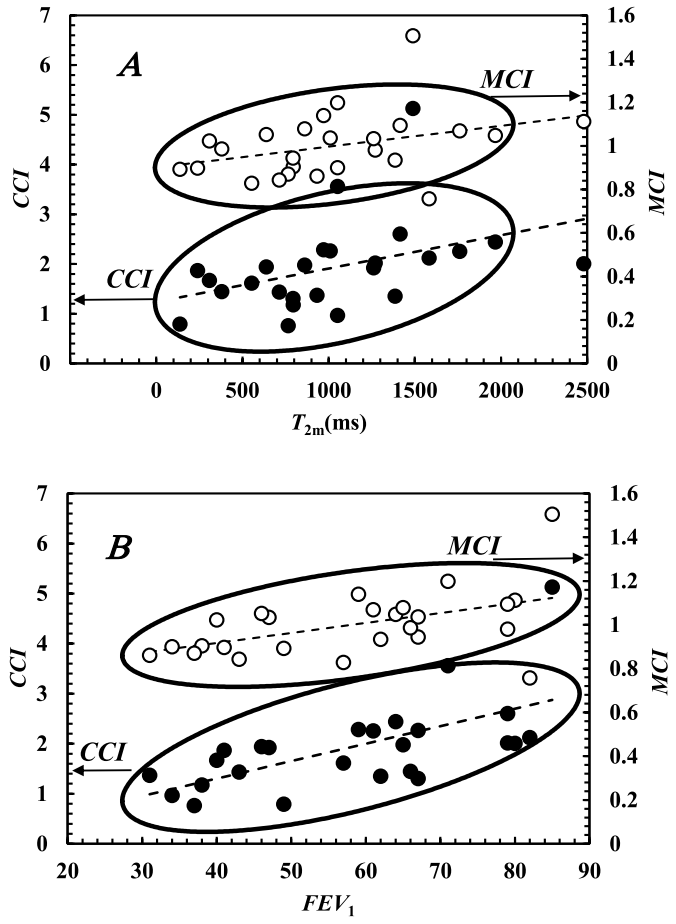

Fig. 5. A) There is a significant direct correlation between CCI (black circles; left vertical axis, see the left oriented arrow) and the average relaxation time T_{2m} ($r_{sp} = 0.56$, $p = 2.5*10^{-3}$; linear interpolant (dashed line) $CCI = (6.7 \pm 3.1)*10^{-4}*T_{2m} + (1.24 \pm 0.36)$); a significant direct correlation between the *MCI* (white circles; right vertical axis, see the right oriented arrow) and the average relaxation time T_{2m} ($r_{sp} = 0.43$, $p = 3.0*10^{-2}$; linear interpolant (dashed line) $MCI = (9.6 \pm 5.3)*10^{-5}*T_{2m} + (0.9 \pm 0.06)$. The solid lines indicate the 95% confidence ellipses. B) There is a significant direct correlation between *CCI* (black circles; left vertical axis, see the left oriented arrow) and FEV_1 ($r_{sp} = 0.68$, $p = 2.0*10^{-4}$; linear interpolant (dotted line) $CCI = (3.5 \pm 0.9)*10^{-2}*FEV_1 + (-0.1 \pm 0.5)$; a significant direct correlation between the *MCI* (white circles, right vertical axis, see the right oriented arrow) and FEV_1 ($r_{sp} = 0.5$, $p = 1.2*10^{-2}$; linear interpolant (dashed line) $MCI = (4.5 \pm 1.7)*10^{-3}*FEV_1 + (0.73 \pm 0.1)$. The solid lines indicate the 95% confidence ellipses.

Interestingly, Fig. 6 indicates that, in most cases (92.5%), ξ spans from about 50 nm to 150 nm, a range in line with literature data on *CF* sputum (≈60–300 nm with average size (140 ± 50) nm) [42,43]. Notably, the combination of rheology and *LF-NMR* is not limited to ξ evaluation as it also allows for the determination of the mesh size distribution ($A_{i\%}$, ξ_i) as depicted in Fig. 7. Indeed, assuming that the three-dimensional network pervading the whole sputum is composed by meshes of different size ξ_i, it can be demonstrated [36–38] that the at each mesh size ξ_i corresponds the relaxation time T_{2i} (see also supporting information S2):

$$\xi_i = \xi\left(\frac{\left(\frac{1}{T_2}\right)_m - \frac{1}{T_{2H2O}}}{\frac{1}{T_{2i}} - \frac{1}{T_{2H2O}}}\right) \quad (1)$$

where T_{2H2O} is the relaxation time of bulk water hydrogen (i.e. water far from polymer chains; ≈ 3700 ms at 37 °C, 20 MHz [44]) and ξ indicates the average mesh size determined by means of rheology. As detailed in the Supporting Information S2, T_{2i} and the relative % abundance $A_{i\%}$ are determined by fitting the experimental relaxation data (see Fig. 3) by means of a sum of exponential terms ($A_{i\%}*\exp(-T_{2i}/t)$; *t* is time).

Fig. 7 refers to a single patient (n. 10, Table 1) for which we have collected three sputum samples over a period time of three months at hospitalization and discharge. At first hospitalization (day 0), 17% of the meshes were 211 nm, 55% 61 nm and 28% 24 nm (see horizontal black bars in Fig. 7).

Thirty days later (discharge), after antibiotic therapy, the percentage of the first class (A_1), characterized by the biggest meshes, were two-fold those of day 0, with a parallel reduction in A_2 and A_3. Altogether, these modifications led to an overall increase in sputum mesh size, which can justify the T_{2m} increase as expected from the data reported in Fig. 6. Notably, also FEV_1 improved, as expected judging from the T_{2m} increase.

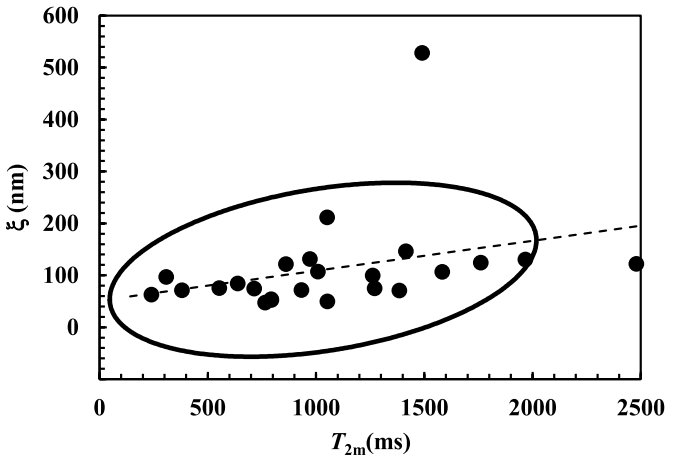

Fig. 6. There is a significant direct correlation between the average mesh size (ξ, black circles) of the sputum polymeric network and the average relaxation time T_{2m} ($r_{sp} = 0.578$, $p = 3.0*10^{-3}$; linear interpolant (dashed line) $\xi = (5.7 \pm 3.3)*10^{-2}*T_{2m} + (51 \pm 39)$. The solid line indicates the 95% confidence ellipses.

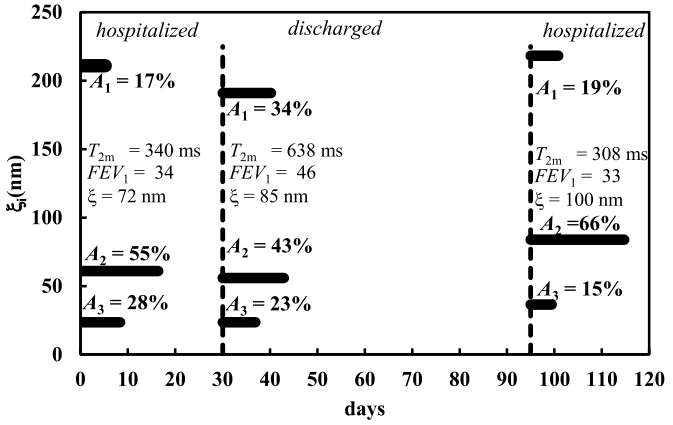

Fig. 7. The time evolution of the mesh size distribution ($A_i - \xi_i$) referring to a single CF patient who was hospitalized and discharged for a three month period (pt. number 10 of Table 1).

Lastly, the patient was hospitalized again on day 95 as there was a decrease in FEV_1 and T_{2m} and A_1 dropped to 19%. This example suggests that not only ξ should be observed but so should the sputum mesh size distribution as it tends to modify over time.

4. Discussion

Herein we have reported further research as to the role T_{2m} plays in the indirect monitoring of *CF* lung disease by demonstrating its correlation with: 1) sputum viscoelasticity, 2) the mucociliary clearability index (*MCI*)/cough clearability index (*CCI*) and 3) average sputum mesh-size. These are all relevant aspects in the airway monitoring of *CF* patients, as respiratory failure is the leading cause of death in these subjects [7]. In order to deeply understand the potentiality of T_{2m} and the rheological parameters considered, it is important recalling some theoretical aspects connected with these parameters. While the determination of solids concentration can provide an exact idea of the sputum hydration, rheology and *LF-NMR* can go further providing also information about the three-dimensional organization of the solid components inside sputum. This is an important aspect, as it is well known that the three-dimensional organization of solid components can heavily affect sputum viscoelastic properties and drug diffusion inside it. In the case of rheology, the combination of the Flory [22] and the equivalent network [27] theories allows to conclude that the shear modulus *G* depends on the mesh size ξ according to:

$$G = \frac{1}{\xi^3}\left(\frac{6RT}{\pi N_A}\right) \quad (2)$$

where N_A is the Avogadro number, *T* is absolute temperature and *R* is the universal gas constant. As ξ depends on both the solid content and on the way solids are interconnected (cross-linked in the case of polymeric chains), it is clear that the rheological characterization is influenced by both solid concentration and solid three-dimensional organization. Only in the case that sputum shows a purely viscous behavior (this means that the elastic modulus *G'* is negligible in comparison to the viscous one *G''* – Fig. 2 demonstrates the opposite behavior for all our samples), the rheological analysis would be essentially affected by solid concentration. Indeed, in this case, the sputum would behave as a solution and not as a gel. Regarding *LF-NMR*, the combined effect of solid concentration and its three-dimensional organization is even more evident. Indeed, in the light of the Fiber cells [37] and the Scherer [45] theories, the relation between the average value of the relaxation time inverse ($(1/T_2)_m$), ξ and the solid volume fraction ϕ reads [38]:

$$\left(\frac{1}{T_2}\right)_m = \frac{1}{T_{2H2O}} + 2\frac{M}{\xi\sqrt{\frac{C_0}{C_1}\frac{1-0.58\phi}{\phi}}} \quad (3)$$

where T_{2H2O} is the free water relaxation time, M is a parameter (relaxivity) accounting for the effect of solid component on the relaxation time of water near the solid surface (bound water), C_0 and C_1 are two constants accounting for network topology (cube, tetrahedron, octahedron). Eq. (2) clearly states that $(1/T_2)_m$ and, thus, T_{2m}, is simultaneously affected by solid concentration (here represented by solids volume fraction ϕ) and by network topology (C_0, C_1 and ξ).

Our data showed that T_{2m} has an inverse correlation with the viscosity (rheological properties) of sputum (Fig. 4A) and that also FEV_1 correlates with its rheological properties (Fig. 4B), evidencing the significance and robustness of the T_{2m} test. The fact that the η_0 correlation with T_{2m}/FEV_1 is less pronounced than that with *G* suggests that the elastic properties of sputum may play a more relevant role than the viscous properties for the evaluation of lung function when correlated to T_{2m} or FEV_1. Moreover, the second relevant finding was that T_{2m} is able to provide reliable information on both *MCI* and *CCI*. Indeed, it was demonstrated that T_{2m} is directly correlated to the rheologically derived *MCI* and *CCI* parameters (Fig. 5A). This may be explained by the fact that a T_{2m} increase implies a reduction of the solid components in the sputum and/or the weakening/disappearance of the three dimensional network that can pervade sputum volume. These features are reflected in the production of a less viscous mucus, which can be more easily removed by *MCI* and *CCI*. Importantly, these data suggest that the complex effect of sputum viscoelastic properties, embodied in *CCI* and *MCI*, is properly summed up by the unique parameter T_{2m}. Notably, in addition to T_{2m}, our data showed that also FEV_1 correlates with *MCI* and *CCI* (Fig. 5B). This is in agreement with our previous observation [9] providing a step forward to the clinical relevance of T_{2m} in *CF* patients.

In order to investigate which of the measured parameters among *G*, η_0 and T_{2m} possesses the strongest linear correlation with FEV_1 (Figs. 4 and 5) a bivariate Principal Component Analysis (*PCA*) was performed as detailed in Supporting Information S3. The results of *PCA* can be summed up by the correlation coefficient $\rho_{X,Y}$. This analysis reveals that *G* ($\rho_{FEV1\text{-}G} = -0.576$) and T_{2m} ($\rho_{FEV1,T2m} = 0.57$) exhibit a similar strong correlation with FEV_1 while a weaker correlation between η_0 ($\rho_{FEV1,\eta0} = -0.162$) and FEV_1 is observed. The same analysis, performed on *MCI* and *CCI* data, indicates a strong direct correlation between *MCI* - FEV_1 ($\rho_{FEV1,MCI} = 0.494$) and *CCI* - FEV_1 ($\rho_{FEV1,CCI} = 0.632$). Thus, among all the considered parameters, *CCI* exhibits the best correlation with FEV_1. These findings are also confirmed by ranking the correlation between

T_{2m}, G, η_0, *MCI* and *CCI* vs FEV_1 according to the absolute value of the Spearman correlation coefficient $|r_{sp}|$. Indeed, we get: *CCI*-FEV_1, $|r_{sp}| = 0.68$; *G*-FEV_1, $|r_{sp}| = 0.63$; T_{2m}-FEV_1, $|r_{sp}| = 0.55$; *MCI*-FEV_1, $|r_{sp}| = 0.5$ and η_0-FEV_1, $|r_{sp}| = 0.41$.

The third important finding in the present investigation is the determination of the correlation between T_{2m} and the average mesh size ξ. Indeed, this parameter has long attracted the attention of researchers due to its relevance on the *CF* sputum/mucus properties [40,46]. In a recent paper [47] it was shown that the average mesh size correlates directly to the elastic modulus. Interestingly, the authors were able to establish a correlation among the average mesh size, the elastic modulus and FEV_1. As they found no correlation between the mucus/sputum solid content and FEV_1, we may presume that the three-dimensional organization (here represented by the average mesh size ξ), rather than the amount of polymers contained in the mucus/sputum, plays the predominant role in determining the lung function of a *CF* patient. Thus, the demonstration of a direct correlation between T_{2m} and the average mesh size (ξ) of the polymeric network pervading the sputum is also relevant from a clinical point of view (Fig. 6). This correlation is in line with the concept that T_{2m} is not only dependent on sputum polymer concentration [8,9] but also on the three dimensional organization of the sputum polymeric network (typically represented by mucins) that determines ξ. This observation may influence therapy as the concentration/spatial organization of pathological substances in the sputum may significantly impair drug efficacy by creating a sort of "shield". Therefore, patients with very low T_{2m} value may well benefit from the administration of muco-active agents. It is important to remind that, theoretically, the determination of ξ could be also performed according to the approximated Scherer theory [45] developed by Abrami [38]:

$$\xi = R_f \sqrt{\frac{C_1}{C_0} \frac{1 - 0.58\phi}{\phi}} \tag{4}$$

while R_f is the radius of the polymeric chains constituting the sputum nanostructure, imagined as an ensemble of interconnected long cylindrical fibers. However, the complex conformation of the different polymeric chains makes very difficult the correct estimation of R_f. Thus, in the case of sputum, we believe that ξ determination is more safely performed by means of rheology (see Supporting Information S1, eqs. S1.3 and S1.4).

Although we only reported one patient with a 3 month follow-up, our data suggest that the different component (A_1-A_2 and A_3) of the mesh size (ξ) can vary over time (Fig. 7). However, further studies are necessary before solid conclusions can be drawn from this preliminary observation, even if our data suggest that the increase in the A_1 component along with the decrease in A_2/A_3 is responsible for T_{2m}/FEV_1 improvement.

As only a small volume of sputum, on average 1–2 ml was tested, it may be that the samples do not accurately reflect the entire lung status. However, some considerations argue against this possibility. Firstly, in line with our previous studies [9] where more than 100 samples were analyzed, a direct correlation between T_{2m}/FEV_1 and T_{2m}/rheological properties of the sputum (Fig. 4A) was observed. This correlation would not be evident if the sample were non-representative. Secondly, the quantity of sputum sampled is in line with that analyzed in recent studies comparing the rheological properties of *CF* sputum with FEV_1 [13,34]. Lastly, it must be remembered that a larger sputum volume cannot be realistically obtained from a patient.

5. Conclusions

T_{2m} measurement is more practical than the widely used FEV_1 to monitor *CF* patients as FEV_1 is highly technique- and effort-dependent. Moreover, compared to FEV_1, T_{2m}: 1) reflects systemic and local inflammation as we have recently reported [8,9]; 2) correlates with sputum viscoelasticity and *MCI*/*CCI*/sputum average mesh-size (this paper), 3) is a quick procedure, i.e., it requires less than 1 min per sample, 4) no special operator training is required, 5) it is very inexpensive (a very good cost/benefit ratio). Therefore, T_{2m} measurement can be performed during routine visits, enabling the clinician to take real time decisions. In addition, T_{2m} shows an important advantage over the determination of the sputum solid concentration. T_{2m} is not only affected by solid concentration (as experimentally demonstrated in our previous paper [8]) but it also depends on the three-dimensional organization of the sputum solid components as theoretically explained at the beginning of the Discussion section. Thus, T_{2m} determination allows to get a picture of the sputum nanostructure that cannot be obtained by the determination of solids concentration.

In conclusion, to the best of our knowledge, this is the first study to use both macro-rheological and *LF-NMR* data in the characterization of *CF* sputum micro- and macro properties. The results herein reported, together with our previous findings, strengthen the significance and the potential utility of T_{2m} for an easy and fast indirect monitoring of lung disease in *CF* patients.

CRediT authorship contribution statement

Michela Abrami: Execution of experimental tests, data fitting and analysis. **Massimo Maschio:** selected the patients, performed FEV1 measurement, provided the clinical data of the patients selected. **Massimo Conese:** originally proposed the research subject, critically discussed the overall data obtained. **Marco Confalonieri:** made available his experience in the pneumology field to discuss the data obtained particularly in relation to the practical use/utility of the method. **Fabio Gerin:** sample data, transferring the samples to the research lab, Formal analysis. **Barbara Dapas:** Formal analysis. **Rossella Farra:** Formal analysis. **Alessandra Adrover:** Formal analysis. **Lucio Torelli:** general planning of the work, coordinated all the activities, Writing – original draft. **Barbara Ruaro:** made available her experience in the pneumology field to discuss the data obtained particularly in relation to the practical use/utility of the method. **Gabriele Grassi:** general planning of the work, coordinated all the activities, Writing – original draft. **Mario Grassi:** general planning of the work, coordinated all the activities and, Writing – original draft.

Declaration of competing interest

All the authors declare that no conflicts of interest exist.

Acknowledgments

This work was supported by the Società Italiana di Reologia –SIR – Italy, by Fondazione Cassa di Risparmio di Trieste, Italy (# 10.3069), and by the so-called "Programma di valorizzazione dei brevetti del sistema universitario del Friuli Venezia Giulia - FVG PoC, 2020, Italy.

References

[1] B. Kerem, J.M. Rommens, J.A. Buchanan, D. Markiewicz, T.K. Cox, A. Chakravarti, M. Buchwald, L.C. Tsui, Identification of the cystic fibrosis gene: genetic analysis, Science 245 (1989) 1073–1080.
[2] D.A. Stoltz, D.K. Meyerholz, M.J. Welsh, Origins of cystic fibrosis lung disease, N. Engl. J. Med. 372 (2015) 351–362.
[3] D.F. Roger, P.G. Barnes, Treatment of airway mucus hypersecretion, Ann. Med. 38 (2006) 116–125.
[4] M.I. Lethem, S.L. James, C. Marriott, J.F. Burke, The origin of DNA associated with mucus glycoproteins in cystic fibrosis sputum, Eur. Respir. J. 3 (1990) 19–23.
[5] C. Fung, S. Naughton, L. Turnbull, P. Tingpej, B. Rose, J. Arthur, H. Hu, C. Harmer, C. Harbour, D.J. Hassett, C.B. Whitchurch, J. Manos, Gene expression of

Pseudomonas aeruginosa in a mucin-containing synthetic growth medium mimicking cystic fibrosis lung sputum, J. Med. Microbiol. 59 (2010) 1089–1100.
[6] R.C. Boucher, Airway surface dehydration in cystic fibrosis: pathogenesis and therapy, Annu. Rev. Med. 58 (2007) 157–170.
[7] D.B. Sanders, R.C. Bittner, M. Rosenfeld, L.R. Hoffman, G.J. Redding, C.H. Goss, Failure to recover to baseline pulmonary function after cystic fibrosis pulmonary exacerbation, Am. J. Respir. Crit. Care Med. 182 (2010) 627–632.
[8] M. Abrami, F. Ascenzioni, E.G. Di Domenico, M. Maschio, A. Ventura, M. Confalonieri, G.S. Digioia, M. Conese, B. Dapas, G. Grassi, M. Grassi, A novel approach based on low-field NMR for the detection of the pathological components of sputum in cystic fibrosis patients, Magn. Reson. Med. 79 (2018) 2323–2331.
[9] M. Abrami, M. Maschio, M. Conese, M. Confalonieri, G.S. Di, F. Gerin, B. Dapas, F. Tonon, R. Farra, E. Murano, G. Zanella, F. Salton, L. Torelli, G. Grassi, M. Grassi, Use of low field nuclear magnetic resonance to monitor lung inflammation and the amount of pathological components in the sputum of cystic fibrosis patients, Magn. Reson. Med. 84 (2020) 427–436.
[10] S. Girod, J.M. Zahm, C. Plotkowski, G. Beck, E. Puchelle, Role of the physiochemical properties of mucus in the protection of the respiratory epithelium, Eur. Respir. J. 5 (1992) 477–487.
[11] UK Cystic Fibrosis Trust, Standards for the Clinical Care of Children and Adults with Cystic Fibrosis in the UK, 2011.
[12] J. Patarin, E. Ghiringhelli, G. Darsy, M. Obamba, P. Bochu, B. Camara, S. Quetant, J.L. Cracowski, C. Cracowski, d.S. Robert, V, Rheological analysis of sputum from patients with chronic bronchial diseases, Sci. Rep. 10 (2020) 15685.
[13] J.T. Ma, C. Tang, L. Kang, J.A. Voynow, B.K. Rubin, Cystic fibrosis sputum rheology correlates with both acute and longitudinal changes in lung function, Chest 154 (2018) 370–377, 18.
[14] M. Stigliani, M.D. Manniello, O. Zegarra-Moran, L. Galietta, L. Minicucci, R. Casciaro, E. Garofalo, L. Incarnato, R.P. Aquino, G.P. Del, P. Russo, Rheological properties of cystic fibrosis bronchial secretion and in vitro drug permeation study: the effect of sodium bicarbonate, J. Aerosol Med. Pulm. Drug Deliv. 29 (2016) 337–345.
[15] E. Puchelle, J.M. Zahm, D. Quemada, Rheological properties controlling mucociliary frequency and respiratory mucus transport, Biorheology 24 (1987) 557–563.
[16] M.J. Dulfano, K.B. Adler, Physical properties of sputum. VII. Rheologic properties and mucociliary transport, Am. Rev. Respir. Dis. 112 (1975) 341–347.
[17] M.S. Zach, The role of recombinant human DNase in the treatment of patients with cystic fibrosis: many promises, more problems, Thorax 51 (1996) 750–755.
[18] E. Odeblad, Measurement of sputum viscosity with the NMR-method, Scand. J. Respir. Dis. Suppl. 90 (1974) 37–39.
[19] C.G. Lofdahl, E. Odeblad, Biophysical variables relating to visco-elastic properties of mucus secretions, with special reference to NMR-methods for viscosity measurement, Eur. J. Respir. Dis. Suppl. 110 (1980) 113–127.
[20] M. King, G. Brock, C. Lundell, Clearance of mucus by simulated cough, J. Appl. Physiol. 58 (1985) 1776–1782.
[21] M. King, Role of mucus viscoelasticity in clearance by cough, Eur. J. Respir. Dis. Suppl. 153 (1987) 165–172.
[22] P. Flory, The thermodynamics of polymer solutions, in: Principles of Polymer Chemistry, 1953, pp. 469–470.
[23] P.G. Bhat, D.R. Flanagan, M.D. Donovan, Drug diffusion through cystic fibrotic mucus: steadystate permeation, rheologic properties, and glycoprotein morphology, J. Pharmacol. Sci. 85 (1996) 624–630.
[24] M. Dawson, D. Wirtz, J. Hanes, Enhanced viscoelasticity of human cystic fibrotic sputum correlates with increasing microheterogeneity in particle transport, J. Biol. Chem. 278 (2003) 50393–50401.
[25] M. Abrami, P. Marizza, F. Zecchin, P. Bertoncin, D. Marson, R. Lapasin, R.F. de, P. Posocco, G. Grassi, M. Grassi, Theoretical importance of PVP-alginate hydrogels structure on drug release kinetics, Gels 5 (2019) 22.
[26] R. Lapasin, S. Pricl, Rheology of Industrial Polysaccharides: Theory and Applications, Blackie, London, 1995, pp. 162–249.
[27] J. Schurz, Rheology of polymer solutions of the network type 16 (1991) 1–53.
[28] J.G. Zayas, G.C. Man, M. King, Tracheal mucus rheology in patients undergoing diagnostic bronchoscopy. Interrelations with smoking and cancer, Am. Rev. Respir. Dis. 141 (1990) 1107–1113.
[29] B. DasGupta, M. King, Reduction in viscoelasticity in cystic fibrosis sputum in vitro using combined treatment with nacystelyn and rhDNase, Pediatr. Pulmonol. 22 (1996) 161–166. 19.
[30] M. King, B. DasGupta, R.P. Tomkiewicz, N.E. Brown, Rheology of cystic fibrosis sputum after in vitro treatment with hypertonic saline alone and in combination with recombinant human deoxyribonuclease I, Am. J. Respir. Crit. Care Med. 156 (1997) 173–177.
[31] M. King, Experimental models for studying mucociliary clearance, Eur. Respir. J. 11 (1998) 222–228.
[32] E.M. App, R. Kieselmann, D. Reinhardt, H. Lindemann, B. DasGupta, M. King, P. Brand, Sputum rheology changes in cystic fibrosis lung disease following two different types of physiotherapy: flutter vs autogenic drainage, Chest 114 (1998) 171–177.
[33] R. Gosselink, G. Gayan-Ramirez, E. Houtmeyers, P.K. de, M. Decramer, High-dose lidocaine reduces airway mucus transport velocity in intubated anesthetized dogs, Respir. Med. 100 (2006) 258–263.
[34] G. Tomaiuolo, G. Rusciano, S. Caserta, A. Carciati, V. Carnovale, P. Abete, A. Sasso, S. Guido, A new method to improve the clinical evaluation of cystic fibrosis patients by mucus viscoelastic properties, PloS One 9 (2014), e82297.
[35] M. Cross, Rheology of non-Newtonian fluids: a new flow equation for pseudoplastic systems, J. Colloid Sci. 20 (1956) 417–437.
[36] K. Brownstein, C. Tarr, Importance of classical diffusion in NMR studies of water in biological cells, Phys. Rev. 19 (1979) (1979) 2446–2453.
[37] M. Chui, R. Phillips, M. Mccarthy, Measurement of the porous microstructure of hydrogels by nuclear magnetic resonance, J. Colloid Interface Sci. 174 (1995) 336–344.
[38] M. Abrami, G. Chirappa, R. Farra, G. Grassi, P. Marizza, M. Grassi, Use of low field NMR for the characterization of gels and biological tissues, ADMET DMPK 6 (2018) 36–46.
[39] S. Meiboom, D. Gill, Modified spin-echo method for measuring nuclear relaxation times, Rev. Sci. Instrum. 29 (2009) 688–691.
[40] S.K. Lai, Y.Y. Wang, D. Wirtz, J. Hanes, Micro- and macrorheology of mucus, Adv. Drug Deliv. Rev. 61 (2009) 86–100.
[41] S. Lustig, N. Peppas, Solute diffusion in swollen membranes. IX. Scaling laws for solute diffusion in gels, J. Appl. Polym. Sci. 36 (1998) (1998) 735–747.
[42] J.S. Suk, S.K. Lai, Y.Y. Wang, L.M. Ensign, P.L. Zeitlin, M.P. Boyle, J. Hanes, The penetration of fresh undiluted sputum expectorated by cystic fibrosis patients by non-adhesive polymer nanoparticles, Biomaterials 30 (2009) 2591–2597.
[43] J.S. Suk, S.K. Lai, N.J. Boylan, M.R. Dawson, M.P. Boyle, J. Hanes, Rapid transport of mucoinert nanoparticles in cystic fibrosis sputum treated with N-acetyl cysteine, Nanomedicine 6 (2011) 365–375.
[44] T. Coviello, P. Matricardi, F. Alhaique, R. Farra, G. Tesei, S. Fiorentino, F. Asaro, G. Milcovich, M. Grassi, Guar gum/borax hydrogel: rheological, low field NMR and release characterizations, Express Polym. Lett. 7 (2013) 733–746.
[45] G.W. Scherer, Hydraulic radius and mesh size of gels, J. Sol. Gel Sci. Technol. 1 (1994) 285–291.
[46] V.Y. Lin, N. Kaza, S.E. Birket, H. Kim, L.J. Edwards, J. LaFontaine, L. Liu, M. Mazur, S.A. Byzek, J. Hanes, G.J. Tearney, S.V. Raju, S.M. Rowe, Excess mucus viscosity and airway dehydration impact COPD airway clearance, Eur. Respir. J. 55 (2020).
[47] G.A. Duncan, J. Jung, A. Joseph, A.L. Thaxton, N.E. West, M.P. Boyle, J. Hanes, J. S. Suk, Microstructural alterations of sputum in cystic fibrosis lung disease, JCI. Insight. 1 (2016), e88198.